Brazilian Journal
of Chemical
Engineering

ISSN 0104-6632
Printed in Brazil
www.abeq.org.br/bjche

Vol. 31, No. 01, pp. 119 - 129, January - March, 2014

STUDY OF MIXING BEHAVIOR OF CSTR USING CFD

D. Rajavathsavai, A. Khapre* and B. Munshi

Department of Chemical Engineering, National Institute of Technology,
Phone: + 91 7894044869, Rourkela, 769008, Orissa, India.
E-mail: akhilesh_khapre@yahoo.co.in

(Submitted: July 8, 2012 ; Revised: March 13, 2013 ; Accepted: March 20, 2013)

Abstract - The continuous stirred tank reactor (CSTR) is a widely used equipment in chemical related industries. The flow behaviour of fluid inside the reactor may either change from dispersion to ideal or ideal to dispersion mixing state. It is studied using the computational fluid dynamics (CFD) simulation software ANSYS Fluent. The mixing behaviour is predicted in terms of age distribution function, $I(\theta)$. For the CSTR without impeller and baffles, $I(\theta)$ is found by the tracer injection method. It is measured and predicted by the impeller swept volume method for the CSTR in the presence of impeller and baffles. The predicted results are found to be in good agreement with the literature experimental data. Effect of rpm of the impeller, Reynolds number and viscosity of the process fluid on the mixing characteristics has been investigated.
Keywords: Computational Fluid Dynamics (CFD); CSTR; Age distribution function; Laminar flow.

INTRODUCTION

The efficiency of heat and mass transfer largely depends on the extent of mixing. If the reactants are premixed, the reaction can start from the entry of the reactor. On the other hand, under non-premixed conditions, reactants must first come in contact and then undergo reaction. Physical phenomena/processes like diffusion, pumping of fluid in the reactor and mechanical agitation control the mixing (http://en. wikipidia.org/wiki/Continuous_reactor). Mixing due to diffusion depends on concentration or temperature gradients. This is commonly observed in micro reactors. In larger reactors, mixing by diffusion is not practically acceptable because of a low rate of mixing. In most cases, the continuous reactors use mechanical agitation for mixing. Because of agitation, efficient mixing can occur irrespective of production capacity and viscosity of the fluid. The mechanical agitator provides better performance of CSTR, giving more conversion of reactant to product.

The mixing performance of a CSTR can be characterized by residence time distribution (RTD) analysis. It provides information on how long the various fluid elements have been in the reactor. As it gives a quantitative measure of the degree of backmixing within a system, knowledge of the liquid RTD is very important for designing a non-ideal reactor (Fogler, 1999). Also, RTD represent a tool in successful process scale-up of chemical reactors. Many researchers have carried out experiments and simulations (Arratia *et al*., 2004; Buflham, 1983; Danckwets, 1953 and 1958; Hocien *et al*., 2008; Levenspiel and Turner, 1970; Levenspiel *et al*., 1970; Martin, 2000; Robinson and Tester, 1986; Trivedi and Vasudeva, 1974; Turner, 1982; Xiao-chang *et al*., 2009; Yablonskya *et al*., 2009; Zwietering, 1959) on RTD of CSTR.

Lipowska (1974) found the RTD of the reactor without and with baffles and moving stirrer. The purpose of his work was to find the tank Reynolds number, which accounts for the inlet energy, sufficient for ideal mixing conditions. He also found the

*To whom correspondence should be addressed

minimum number of impeller rotations required to reach ideal mixing in the moving stirrer case. For ideal mixing of the liquid solely by the inlet energy, the following relations must be obeyed (Burghardt and Lipowska, 1972):

$$Re = \frac{4V^*\rho}{\pi D\mu} \geq 13.5 \quad (1)$$

where Re is the tank Reynolds number based on the tank diameter D, and ρ and μ are the liquid density and viscosities, respectively; V^* is the inlet volumetric flow rate. Eq. (1) was developed for fixed diameters of the tank and inlet. Therefore, in terms of inlet diameter, d, the inlet Reynolds number, Re_{in} can be written as:

$$Re_{in} = \frac{Re}{d/D} = \frac{4V^*\rho}{\pi d\mu} \geq 347 \quad (2)$$

Lipowska (1974) extended the work of Burghardt and Lipowska (1972) to determine the dependency of Re and Re_{in} on the d/D ratio. The equations are:

$$Re \geq 569.1\left(\frac{d}{D}\right)^{1.09} \quad (3)$$

$$Re_{in} \geq 569.1\left(\frac{d}{D}\right)^{0.09} \quad (4)$$

The above equation shows little effect of d/D ratio on Re_{in}. The equations allow us to calculate the minimum inlet volumetric flow necessary for the ideal mixing of liquid without stirrer.

In the case of mixing with a mechanical stirrer, the number of revolutions needed for ideal mixing can be evaluated from:

$$N = 2428.2\ Re^{-1.215}\left(\frac{d}{D}\right)^{0.088} \quad (5)$$

and the correlations for impeller Reynolds number, Re_m for ideal mixing is

$$Re_m = \frac{N d_m^2 \rho}{\mu} = 269.8\ Re^{-0.215}\left(\frac{d}{D}\right)^{0.088} \quad (6)$$

The foregoing discussion shows that Lipowska (1974) predicted experimentally and uniquely the mixing behaviour in terms of swept volume. This demands a theoretical study so that the swept volume of impeller can be used as a design parameter to calculate RTD of CSTR with different kinds of impeller. In view of this, extensive results of a CFD study of RTD of CSTR are reported in the present communication for a range of swept volume due to variation in speed of the impeller. The work covered here also includes a systematic study of the effect of impeller speed, viscosity of tank liquid and tank Reynolds number on RTD of CSTR. The RTD of CSTR without impeller is also studied numerically by observing the tracer (potassium chloride, KCl) concentration with time at the tank exit. The distribution of KCl in the CSTR is obtained as a function of tank Reynolds number for better understanding the nature of RTD of CSTR. Although the present study focuses on mixing in terms of RTD of CSTR, complementary evaluation of the hydrodynamic behaviour helps to understand it better.

CSTR GEOMETRY SPECIFICATION

A flat bottom baffled agitated vessel with a six bladed turbine disk impeller (Rushton turbine) used in the experiments by Lipowska (1974) is shown schematically in Figure 1. The CSTR is fitted with four symmetric baffles at a 90° interval against the tank wall. The dimensions of the tanks are given in Table 1. The working fluid is a water-glycerin solution and the properties of the solutions are given in Table 2 and Table 3.

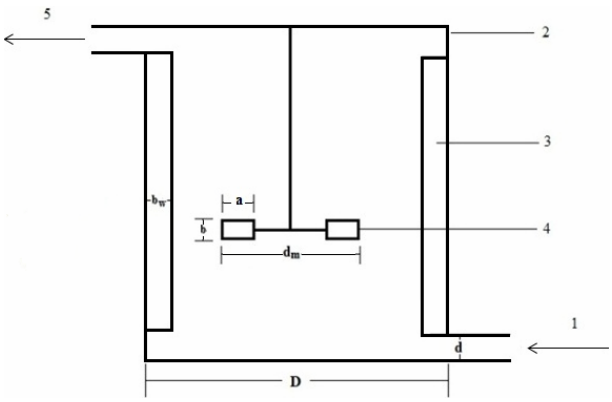

Figure 1: Schematic diagram of the CSTR: (1) Inlet; (2) Reactor Tank; (3) Baffles; (4) Impeller; (5) Outlet.

Table 1: Dimensions of the CSTR.

Sr. No.	Parameters	Values
1	Tank diameter, D	0.099, 0.172, 0.250 m
2	Inlet diameter, d	0.002, 0.0072, 0.0088 m
3	No of baffles	4
4	Baffles width (b_w)	D/12
5	Type of stirrer	Turbine disc impeller
6	Number of blades in the impeller	6
7	Ratio of impeller to the tank diameter	(d_m/D)=1/3
8	Length of the impeller blade, a	(d_m/4)
9	Height of the impeller blade, b	d_m/5
10	Clearance, C	d_m
11	Height of liquid, H	D

Table 2: Parameters used for the CSTR without stirrer and baffles.

Sr. No.	D (m)	d (m)	μ (cp)	ρ (kg/m^3)	V* (l/hr)	τ (min)	Type of Flow
1	0.099	0.002	1	1000	0.621	72.6	Dispersion
2	0.099	0.002	1	1000	1.028	44.86	Dispersion
3	0.099	0.002	1	1000	1.563	29.33	Dispersion
4	0.099	0.002	1	1000	1.922	24.84	Ideal
5	0.250	0.002	7.75	1141	12.82	57.44	Dispersion
6	0.250	0.002	7.75	1141	12.30	61.07	Dispersion
7	0.250	0.002	7.75	1141	17.42	42.27	Ideal

Table 3: Parameters used for the CSTR with stirrer and baffles.

Sr. No.	D (m)	d (m)	μ (cp)	ρ (kg/m^3)	V* (l/hr)	τ (min)	N (rpm)	Type of Flow
1	0.099	0.0072	9.2	1150	2.653	20.46	50	Dispersion
2	0.099	0.0072	9.2	1150	2.653	20.46	70	Dispersion
3	0.099	0.0072	9.2	1150	2.524	18.11	80	Ideal
4	0.099	0.0072	9.2	1150	2.524	18.11	90	Ideal
5	0.172	0.002	9.8	1183	12.24	19.58	20	Dispersion
6	0.172	0.002	9.8	1183	12.56	19.04	30	Dispersion
7	0.172	0.002	9.8	1183	12.56	19.04	35	Ideal
8	0.250	0.0088	19.7	1179	16.42	44.83	12	Dispersion
9	0.250	0.0088	19.7	1179	16.50	44.60	20	Dispersion
10	0.250	0.0088	19.7	1179	16.50	44.60	25	Ideal
11	0.250	0.0088	19.7	1179	16.50	44.60	40	Ideal

In ANSYS FLUENT, the default method of solution of the equations is in a stationary reference frame. However, some problems can be solved advantageously in a moving reference frame where the whole computational domain moves, called a single reference frame approach. But for more complex problems, it is necessary to use Multiple Reference Frame (MRF) with the combination of stationary and moving reference frame. Here, the computational domain is divided into moving and stationary zones with well defined interfaces between the zones. The quantities such as velocity, pressure etc. are exchanged across the interface between the zones. The transient behaviour of moving part systems can be captured by a sliding mesh approach under the MRF model. The moving zone includes stirrer and rotates with the same speed as the stirrer. The stationary zone includes the rest of the control volume comprised of baffles, tank and fluid inside the CSTR. The geometry and mesh are prepared in the ANSYS workbench and shown in Figure 2 (a) and (b). The complicated CSTR geometry is meshed using an unstructured tetrahedral mesh. There are three ways, namely coarse, medium and fine mesh, to develop an unstructured mesh. The fine unstructured mesh is used finally to make sure of the stability and accuracy of the computed results. The unstructured tetrahedral mesh with 735231, 814782 and 874273 cells, covering the whole volume of the tanks with 0.099 m, 0.172 m and 0.250 m diameter, respectively, was used in the simulation work. As expected, a dense mesh at the inlet, outlet of the tank and nearer to the stirrer surface are observed in Figure 2 (b).

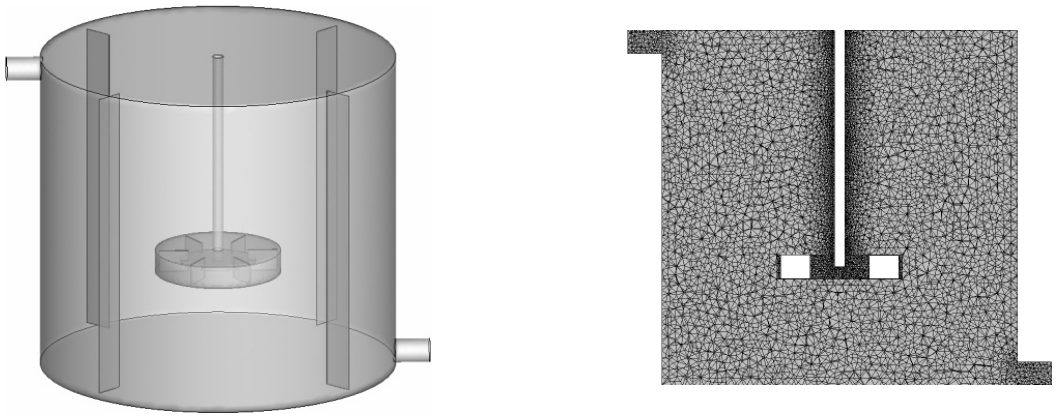

(a) (b)

Figure 2: (a) Computational domain; (b) Computational Mesh.

GOVERNING EQUATIONS AND SOLUTION ALGORITHM

The flow prediction procedure is based on the numerical solution of the three dimensional, time-dependent continuity and momentum equations. The general conservation of mass or continuity can be written as follows (ANSYS FLUENT 12 Theory guide, 2009):

$$\frac{\partial \rho}{\partial t} + \nabla.\left(\rho \vec{\upsilon}\right) = 0 \tag{7}$$

where $\vec{\upsilon}$ is the velocity vector.

The Navier Stokes equations is given as

$$\frac{\partial}{\partial t}\left(\rho \vec{\upsilon}\right) + \nabla.\left(\rho \vec{\upsilon}\vec{\upsilon}\right) = -\nabla p + \nabla.\left(\bar{\bar{\tau}}\right) + \rho \vec{g} + \vec{F} \tag{8}$$

where p is the static pressure and $\bar{\bar{\tau}}$ is the stress tensor (Eq. (9)); $\vec{g}$ and $\vec{F}$ are the gravitational body force and external body forces respectively. The stress tensor $\bar{\bar{\tau}}$ is given by:

$$\bar{\bar{\tau}} = \mu\left[\left(\nabla \vec{\upsilon} + \nabla \vec{\upsilon}^{T}\right) - \frac{2}{3}\nabla.\vec{\upsilon} I\right] \tag{9}$$

where μ is the molecular viscosity, I is the unit tensor, and the second term on the right hand side is the effect of volume dilatation.

Simulation of mixing was carried out by introducing a secondary liquid as an inert tracer into the primary liquid in the vessel. The temporal and spatial distributions of the tracer concentration were obtained from the solution of the species transport equation. This equation for a non-reacting mixture can be expressed in the following form:

$$\frac{\partial}{\partial t}\left(\rho \omega_k\right) + \frac{\partial}{\partial x_j}\left(\rho u_j \omega_k\right) = \frac{\partial}{\partial x_j}\left(\rho D_{eff}\frac{\partial \omega_k}{\partial x_j}\right) \tag{10}$$

where ω_k is the mass fraction of the k^{th} species and D_{eff} is the effective diffusivity of the species in the mixture.

Lipowska (1974) used a step change of potassium chloride (KCl) concentration in the feed to find the RTD of CSTR. But he did not specify the value of concentration of KCl in the feed stream. Thus, it becomes difficult to guess it exactly. Fortunately, the expression for the RTD function, $I(\theta)$ (internal age distribution function), for the moving impeller CSTR is given as:

$$I(\theta) = \exp\left[-\left(\frac{V^*}{Q} + 1\right)\theta\right] \tag{11}$$

where $\theta = t/\tau$, τ is the holdup time of liquid in the tank, V^* is the inlet volumetric flow rate, Q is the impeller pumping capacity.

$$Q = 2.3 N d_m^2 b \ \text{cm}^3/\text{sec} \tag{12}$$

where N is the rpm of the impeller. According to Eq. (11), mixing is ideal when $V^*/Q \to 0$.

In general, the expression of Q for impeller is (Mishra *et al*., 1998):

$$Q = 2\pi \int_{0}^{D/2} \left(r\nu_z\right)\Big|_{z_1} dr + \pi D \int_{z_1}^{z_2} \nu_r \Big|_{D/2} dz \qquad (13)$$

where D, ν_r and ν_z are respectively impeller diameter, radial velocity, and axial velocity; z_1 and z_2 are the boundaries of the impeller-swept volume in the axial direction.

The time constant or holdup time of the reactor, τ, is defined as

$$\tau = \frac{V}{V^*} \qquad (14)$$

The above equation is used to find the liquid volume, V, inside the reactor for a given τ.

The inlet volumetric flow rate is evaluated from $V^* = A_{in}u_{in}$, where A_{in} is the inlet normal cross sectional area and u_{in} is the net inlet velocity.

In CSTR without stirrer and baffles, the definition of Q is not valid. Hence, different KCl concentrations in the feed are taken in the simulation for finding $I(\theta)$ using the following expression:

$$I\left(\theta\right) = \frac{C_0^+ - C\left(t\right)}{C_0^+ - C_0^-} \qquad (15)$$

where the KCl concentration in the inlet changes from C_0^- to C_0^+, and $C\left(t\right)$ is the concentration of KCl in the outlet at any time, t. The molecular diffusivity of KCl in the solution is taken as 1.95 x 10^{-9} m^2/s (Harned and Nuttall, 1949).

In the simulation work, laminar flow with the MRF model is used. The governing equations for the axial, radial and tangential velocities; and the tracer concentration (c) are discretized using the finite-volume method. The convective terms of the governing equations are discretized using a first order upwind differencing scheme. The transient terms are discretized using a first order implicit scheme. A no-slip boundary condition is used for all the solid surfaces. Velocity at the inlet is specified. At the exit of the CSTR, the gauge pressure is taken as zero. The rotation of the impeller is specified. The operating condition of the system is 293 K and 101325 Pa. Finally, the discretized Navier–Stokes equations coupled with a pressure correction equation are solved, together with the discretized equations for tracer component balance equation, iteratively using the SIMPLE (Semi-Implicit Method for Pressure-Linked Equation) algorithm and Gauss-Seidel iterative method (ANSYS FLUENT 12 Theory guide, 2009). The hydrodynamics equations of CSTR without KCl species are solved first by steady state solver to achieve an initial hydrodynamic condition for the transient solver. Under convergence of hydrodynamics equations, KCl is introduced in the tank by a step change. The mass fraction equations for KCl along with the hydrodynamic equations are then solved by the unsteady state method using the previously calculated steady state initial condition. The time increment is taken as 10^{-3} second, and 30 iterations per time step, which is enough to achieve a converged solution at each time step, are taken in the simulation. All dependent variables are modified by the under relaxation method, and used in the next iteration until the solutions converged. The values of under-relaxation factors for pressure, momentum, density, body forces and KCl mass equations are 0.3, 0.7, 1.0, 1.0 and 1.0, respectively. The convergence criteria, i.e., residual of all the discretized equations, are satisfactorily taken as 10^{-3}, and no further change in the results was observed with further reduction of the residual value. An overall mass balance is checked at each time step. In the computations, the inlet flow rates and rotation of the impeller are changed from lower to higher values until the computed $I(\theta)$ matches with the ideal mixing line, $exp\left(-\theta\right)$.

RESULTS AND DISCUSSION

Study on Mixing without Stirrer and Baffles

The contours of tracer concentration throughout the reservoir along time are very interesting because they provide a good perspective on the evaluation of the concentration fronts. The concentration of KCl at the outlet of the tank is measured for a range of its mass fraction from 10^{-4} to 10^{-6} at the inlet.

Potassium chloride (KCl) is injected into the tank as tracer and its concentration is noted with time at the outlet. Using the parameters given in Table 2, the computations are carried out with very low inlet concentration of KCl with mass fraction in the range of 10^{-4} to 10^{-6}. For CSTR without impeller and baffles, contours of mass fraction of KCl at different times are shown in Figure 3. The comparison reveals that KCl reaches closer to the outlet with an increase in *Re*. This happens due to jet-like movement of KCl with inlet fluid towards the opposite wall, and then its movement up along the wall surface. Due to the increase in inlet energy with *Re*, the homogeneity of the liquid in CSTR increases.

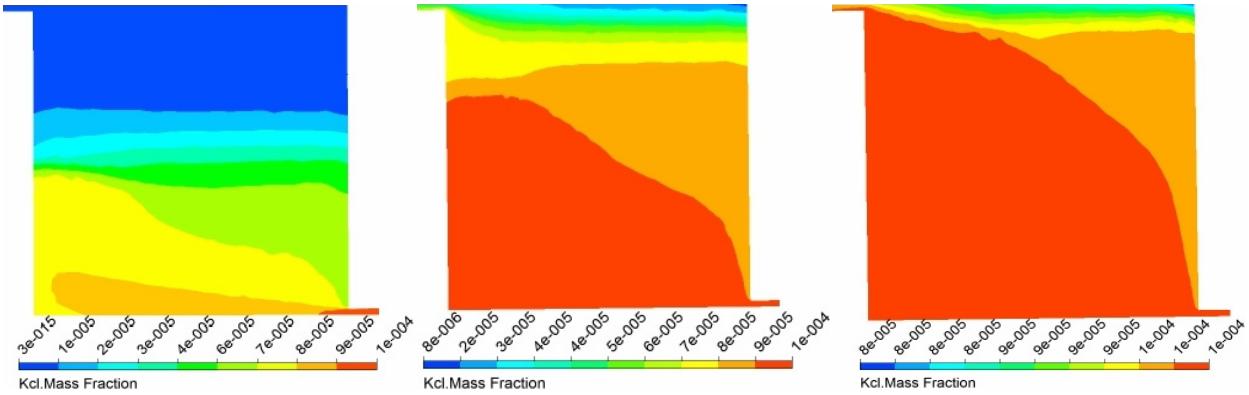

(i) at θ = 0.4 (ii) at θ = 1 (iii) at θ = 2

Figure 3: (a) The contours of KCl mass fraction for Re = 2.25, D = 0.099 m, d = 0.002 m, μ = 1 cP and ρ = 1000 kg/m^3 for the CSTR without impeller; (i) θ = 0.4, (ii) θ = 1, (iii) θ = 2

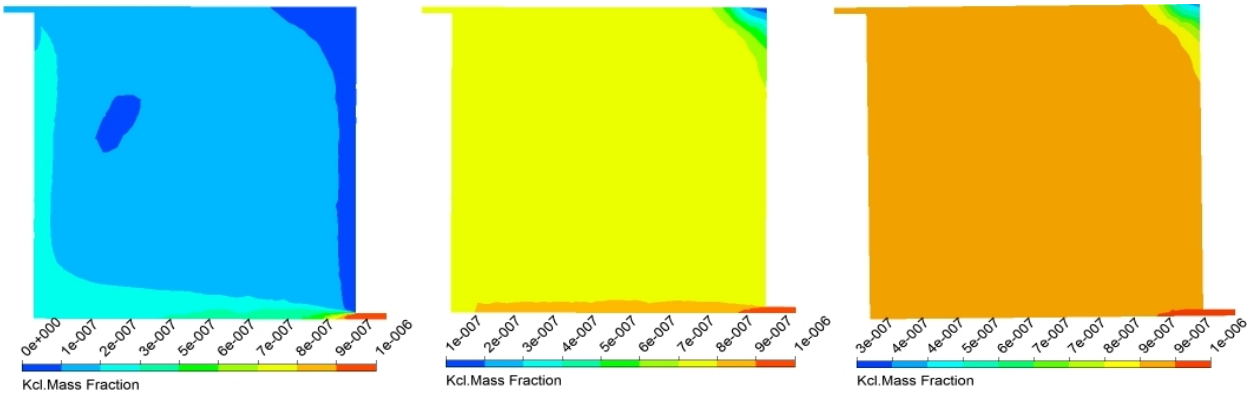

(i) at θ = 0.4 (ii) at θ =1 (iii) at θ = 2

Figure 3: (b) The contours of KCl mass fraction for Re = 5.57, D = 0.099 m, d = 0.002m, μ = 1 cP and ρ = 1000 kg/m^3 for the CSTR without impeller; (i) θ = 0.4, (ii) θ = 1, (iii) θ = 2.

The mixing behaviour is quantitatively predicted by $I(\theta)$. It is calculated by Eq. (15) using the simulated exit concentration of KCl at the outlet of the CSTR. The predicted $I(\theta)$ are compared with both the experimental data of Lipowska (1974) and the ideal mixing line. These are depicted in Figure 4 and Figure 5, and also tabulated in Table 2. The results show an excellent agreement with the experimental results. The analysis reveals that, with increasing tank Reynolds number (Re), the hydro-dynamics of CSTR approaches dispersion flow to the ideal mixing state. If KCl enters the tank through a larger diameter inlet, it spreads more in the bulk liquid inside the tank compared to the lower diameter inlet. Therefore, the system approaches the ideal mixing state at a much lower value of the Reynolds number as the inlet tube diameter increases from 0.002 m to 0.0088 m.

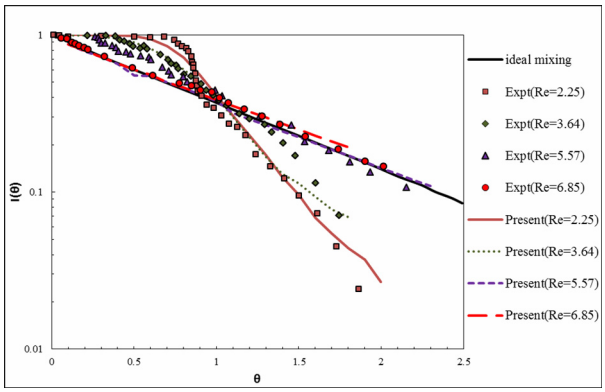

Figure 4: Plot of $I(\theta)$ vs. θ for a CSTR without stirrer and baffles and with D = 0.099 m, d = 0.002 m, μ = 1 cP and ρ = 1000 kg/m^3. The KCl inlet mass fraction, for Re = 2.25 and 3.64 is 10^{-4}; for Re = 5.57 is 10^{-5}; for Re = 6.85 is 10^{-6}.

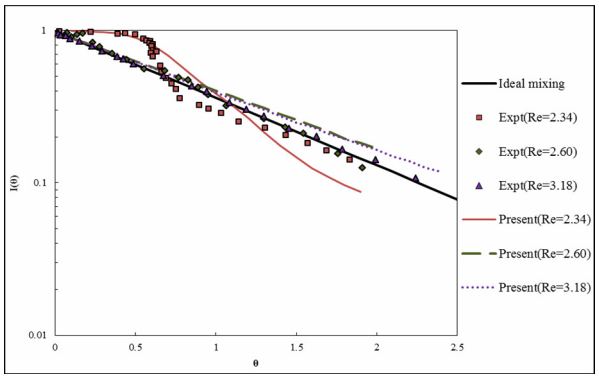

Figure 5: Plot of $I(\theta)$ vs. θ for a CSTR without stirrer and baffles and with D = 0.250 m, d = 0.0088 m, μ = 7.75 cP and ρ = 1000 kg/m^3. The KCl inlet mass fraction, for Re = 2.34 and 2.60 is 10^{-4}; for Re = 3.18 is 10^{-6}.

Study on Mixing with Stirrer and Baffles

For the moving impeller case, the resulting velocity distributions in the radial direction at different axial positions are shown in Figure 6.

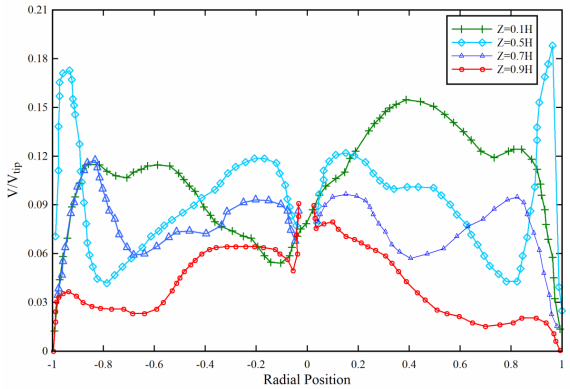

(a)

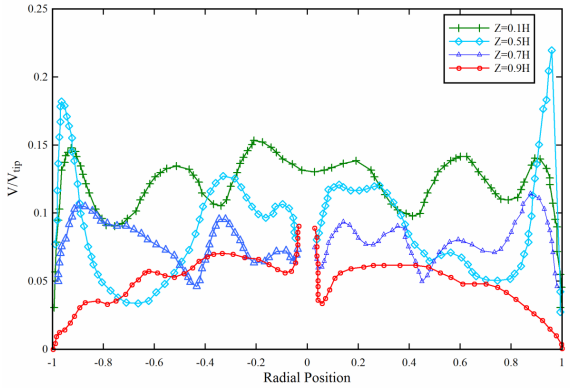

(b)

Figure 6: Velocity profile with radial position at different axial positons for a CSTR with moving impeller and baffles, for D = 0.099 m, d = 0.0072 m, μ = 9.2 cP and ρ = 1145 kg/m^3; (a) N = 50 rpm, (b) N = 90 rpm.

At the bottom surface of the CSTR, Z is 0. The velocities are normalized by the impeller tip velocity ($V_{tip} = \pi ND$). The rotation of the impeller in the tank forms a typical double loop circulation. An effect of impeller speed on the velocity profiles at different tank diameter is clearly visible. The inlet to the CSTR is positioned closer to the stirrer and, hence, more asymmetry in the flow field is observed closer to the impeller surface. An increase in symmetry in the velocity profile is observed at higher axial position. This happens because of the mechanical energy imparted by the impeller superseding the inlet flow energy. The interaction of inlet fluid energy with impeller energy results in more mixing of the fluid. A maximum velocity is observed nearer the right wall of the tank and just above the impeller. This occurs due to the presence of the inlet on the same side and also due to the appearance of stronger recirculation above the impeller. The velocity profile ensures the proportionate variation of local velocities with impeller speeds. Nearer to the top surface, the maximum velocity is obtained nearer the rotating shaft surface.

A comparison of the Fluent predicted $I(\theta)$ and that measured experimentally by Lipowska (1974) obtained by the tracer injection method is presented graphically in Figures 7, 8 and 9 for different rpm. Eq. (12) shows that the value of Q is constant for a particular impeller with fixed angular motion. Thus, the value of V^*/Q is also constant for a particular run. Therefore, the variation of $I(\theta)$ with θ should be linear on a semi-log graph. The linear variation is also observed in the present work. At lower impeller speed, the mismatch between the experimental data and the present values is obvious. But a careful observation shows that the computed values can predict the nature of fluid mixing perfectly, as mentioned in Table 3. According to Eq. (11), $I(\theta)$ becomes ideal mixing internal age distribution function as V^*/Q tends to zero. This may be possible by increasing the rpm of the impeller. Therefore, the computed $I(\theta)$ approaches the ideal mixing line with the increase in impeller rotation (N) and the graphs depict that, at higher values of N, the CFD results are in excellent agreement with the experimental data. In the figures it is also noticed that, at the initial moment, there is a transient Q up to a certain θ, and hence there is a relatively better agreement of the computed $I(\theta)$ with the experimental data. The study also shows that the required rpm of the impeller decreases to reach the ideal mixing state with an increase in diameter of the vessel.

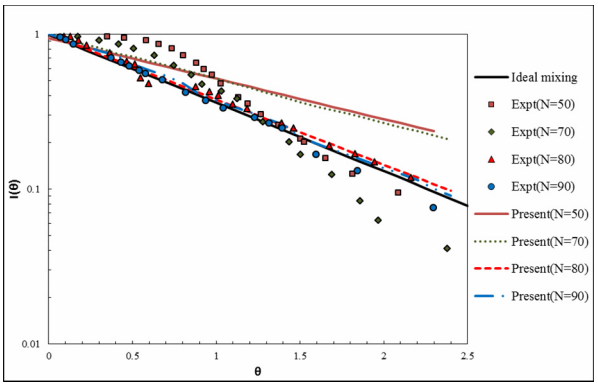

Figure 7: Plot of $I(\theta)$ vs. θ for a CSTR with stirrer and baffles and with D = 0.099 m, d = 0.0072 m, μ = 9.2 cP and ρ = 1145 kg/m^3.

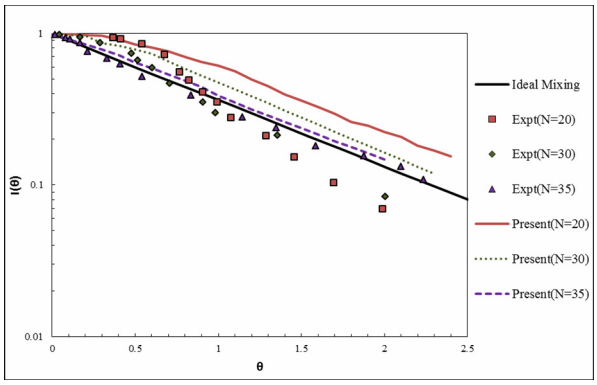

Figure 8: Plot of $I(\theta)$ vs. θ for a CSTR with stirrer and baffles and with D = 0.172 m, d = 0.002 m, μ = 9.8 cP and ρ = 1163 kg/m^3.

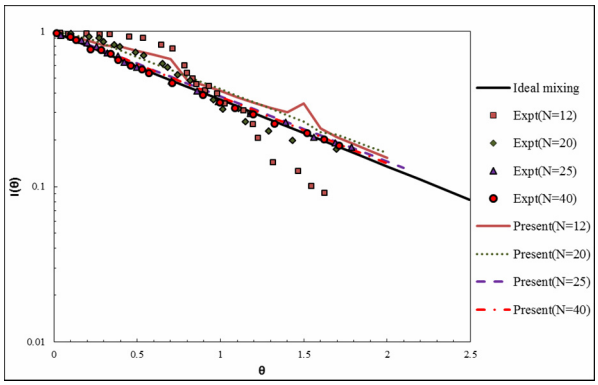

Figure 9: Plot of $I(\theta)$ vs. θ for a CSTR with stirrer and baffles and with D = 0.250 m, d = 0.0088 m, μ = 19.7 cP and ρ = 1179 kg/m^3.

Effect of Tank Reynolds Number, Impeller Rotation and Viscosity of the Liquid on the Mixing

Simulations have been carried out to examine the influence of parameters on $I(\theta)$ and also to carry out a qualitative comparison of the mixing behaviour. The effect of *Re*, N and fluid viscosity on the mixing behavior of the liquid in a CSTR is studied. Figure 10 represents the effect of *Re* on $I(\theta)$ at constant impeller rotation, $N = 50$ rpm. At *Re* 0.98, dispersion flow occurs, at *Re* 1.03 the mixing line goes relatively closer to ideal mixing line, and further increase in *Re* to 1.5 and then to 2.03 results in the mixing line following the ideal mixing line. The energy of the inlet flow increases with an increase in V^*, which increases proportionately with *Re*. This inlet energy helps to mix the liquid. Therefore, $I(\theta)$ approaches the ideal mixing line with an increase in *Re* as observed in Figure 8.

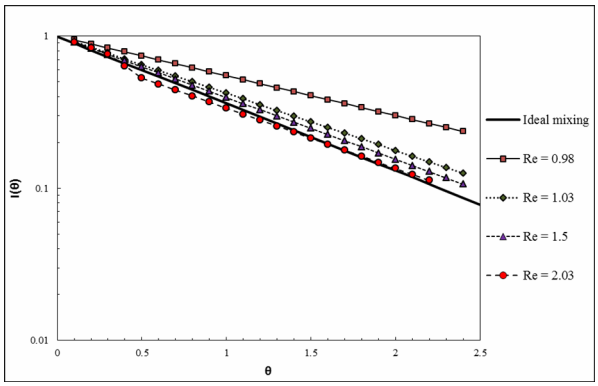

Figure 10: Effect of tank Reynolds number, *Re* on $I(\theta)$ for a CSTR with stirrer and baffles and with D = 0.099 m, d = 0.0066 m, N = 50 rpm, μ = 9.2 cP.

The effect of impeller rpm on the mixing efficiency is demonstrated in Figure 11. It can be observed that the nature of the flow changes from

dispersion to an ideal mixing state with the increase in N. A distinct dispersion flow happens at N equal to 30 and 40 (these two curves are superimposed), and also at 50, whereas at $N = 80$ the mixing is very near to the ideal mixing condition. This happens naturally as it is well known that the amount of mechanical energy imparted to the fluid increases with an increase in N, and hence more mixing.

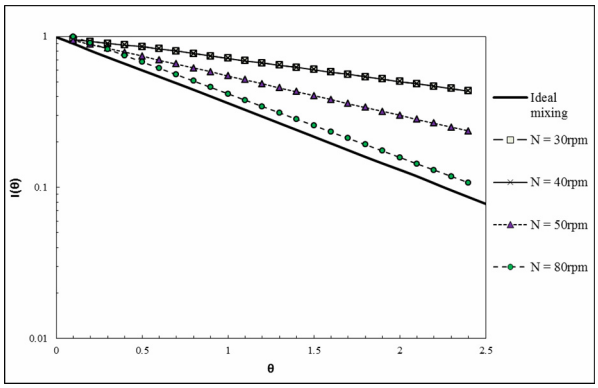

Figure 11: Effect of N on $I(\theta)$ for a CSTR with stirrer and baffles and with D = 0.250 m, d = 0.0066 m, μ = 9.2 cP, ρ = 1145 kg/m^3 and Re = 1.03.

Viscosity of the fluid has a certain effect on the hydrodynamic and mixing behavior of the liquid. The effect of viscosity of the liquid on $I(\theta)$ at different impeller speeds is shown in Figure 12. The effect of viscosity on $I(\theta)$ at high N is just the reverse of the effect observed at lower values of N. Figure 12 (c) and (d) show that the mixing of the liquid moves towards the ideal mixing state with an increase in viscosity at rpm 50 and 70, whereas it moves away from the ideal mixing line for rpm 25 and 12 as observed in Figure 12 (a) and (b). For a particular Re, V^* increases with viscosity. In addition to this, the impeller does more mechanical work at higher values of N, and it makes the viscous force negligible. Thus, the increase of V^* results in more mixing of the liquid in CSTR. The mixing of liquid therefore moves towards the ideal mixing condition at higher impeller rotation. But at lower values of N, the amount of energy transferred by the impeller to the liquid is relatively low, and it becomes insufficient to overcome the viscous force. Due to domination of the viscous force at lower N, the mixing line moves away from the ideal mixing line.

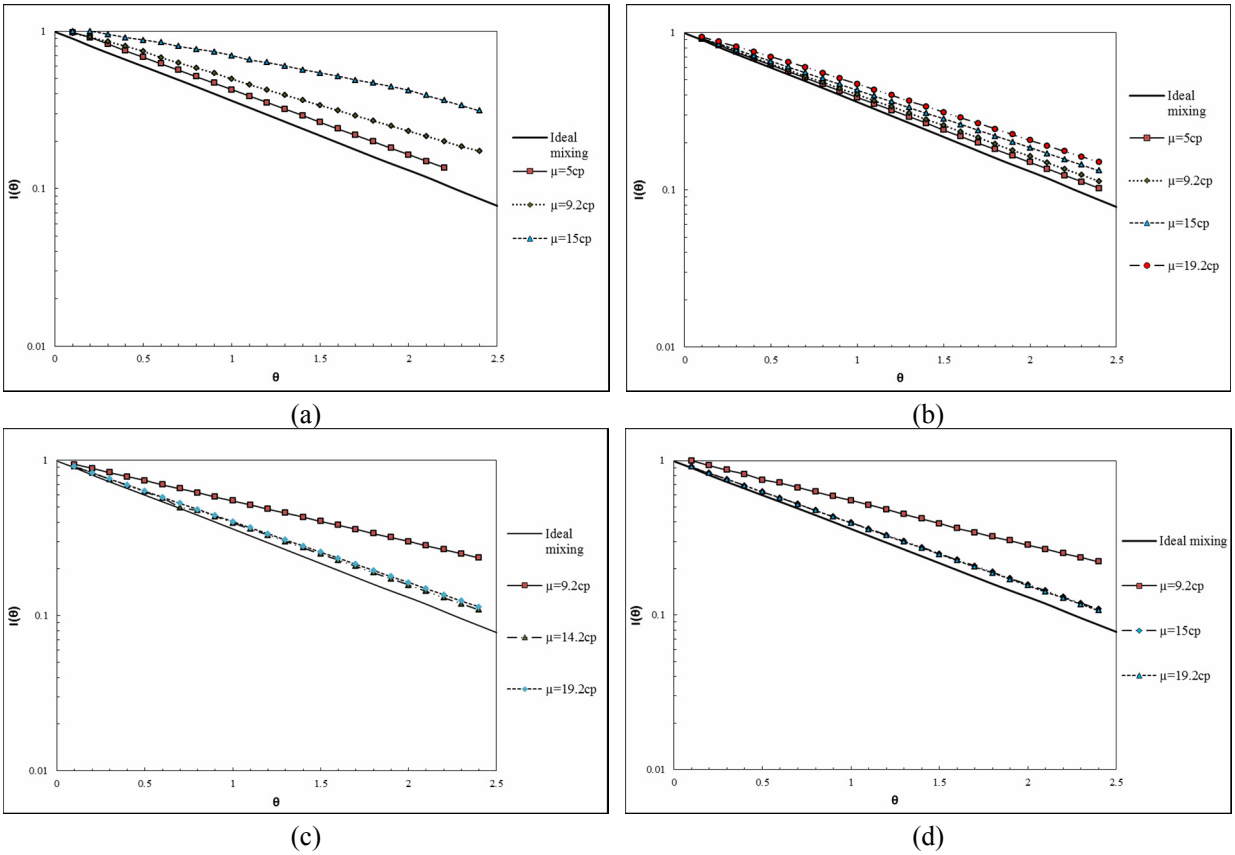

Figure 12: Effect of viscosity of the liquid on $I(\theta)$ for a CSTR with stirrer and baffles with D = 0.099 m, d = 0.0066 m, Re = 1.03: (a) N = 10 rpm; (b) N = 25 rpm; (c) N = 50 rpm and (d) N = 70 rpm.

CONCLUSION

CFD simulations have been carried out successfully to predict the mixing behavior of liquid in a CSTR. The conclusions may be summarized as follows:

1. The mixing predictions have been found to be in good agreement with the experimental results available in the open literature.
2. The simulation results prove that the swept volume of the impeller can be used to predict $I(\theta)$ of the CSTR with impeller and baffles.
3. Effects of rpm of the impeller, tank Reynolds number (Re) and viscosity of the liquid on $I(\theta)$ have been investigated.
4. The mixing behaviour has been found to move from dispersion to ideal mixing as the rpm (N) of the impeller increases. The effect of the viscosity of the liquid on the mixing has been found to be rpm dependent.

NOMENCLATURE

a	Length of the impeller blade	m
A	Cross sectional area	m^2
b	Height of the impeller blade	m
b_w	Baffle width	m
C_0^+	Concentration of a tracer fed into the reactor after a step-wise change	mole/L
C_0^-	Initial concentration of a tracer in the reactor	mole/L
$C(t)$	Concentration of a tracer at an outlet from the reactor at the moment t	mole/L
D	Tank diameter	m
d	Inlet tube diameter	m
d_m	Impeller diameter	m
H	Height of liquid tank	m
N	Impeller speed	RPM
Q	Impeller pumping capacity	m^3/min
Re	Tank Reynolds number	(-)
Re_m	Impeller Reynolds number	(-)
Re_{in}	Inlet Reynolds number	(-)
t	Time	min/sec
u_{in}	Inlet velocity	m/sec
V	Tank volume	m^3
V^*	Volumetric flow rate	l/hr/m^3/sec
V_{tip}	Impeller tip velocity	m/sec

Greek Symbols

τ	Time constant	(-)
μ	Viscosity	cP
ρ	Density	kg/m^3
θ	Dimensionless time	(-)
σ	Variance of the residence time distribution	(-)

REFERENCES

ANSYS FLUENT 12.0 Theory Guide, ANSYS Inc. (2009).

Arratia, P. E., Lacombe, J. P., Shinbrot, T. and Muzzio, F. J., Segregated regions in continuous laminar stirred tank reactors. Chemical Engineering Science, 59, 1481-1490 (2004).

Buflham, B. A., Internal and external residence-time distributions. Chemical Engineering Communications, 22, 105-107 (1983).

Burghardt, A. and Lipowska, L., Mixing phenomena in a continuous flow stirred tank reactor. Chemical Engineering Science, 27, 1783-1795 (1972).

Continuous Reactor, Wikipedia, the Free Encyclopedia, Wikimedia Foundation Inc. (2004). http://en.wikipidia.org/wiki/Continuous_reactor.

Danckwerts, P. V., Continuous flow systems: Distribution of residence times. Chemical Engineering Science, 2, 1-13 (1953).

Danckwerts, P. V., The effect of incomplete mixing on homogeneous reactions. Chemical Engineering Science, 8, 93-102 (1958).

Fogler, H. S., Elements of Chemical Reaction Engineering. 3rd Ed., Pearson Education Inc., New Jersey (1999).

Harned, H. S. and Nuttall, R. L., The differential diffusion coefficient of potassium chloride in aqueous solutions. Journal of the American Chemical Society, 71, 1460-1463 (1949).

Hocine, S., Pibouleau, L., Azzaro-Pantel, C. and Domenech, S., Modelling systems defined by RTD curves. Computers & Chemical Engineering, 32, 3112-3120 (2008).

Levenspiel, O. and Turner, J. C. R., The interpretation of residence-time experiments. Chemical Engineering Science, 25, 1605-1609 (1970).

Levenspiel, O., Lai, B. W. and Chatlynne, C. Y., Tracer curves and the residence time distribution. Chemical Engineering Science, 25, 1611-1613 (1970).

Lipowska, L., The influence of geometric parameters on the ideal mixing range of liquid in a continuous flow stirred tank reactor. Chemical Engineering Science, 29, 1901-1908 (1974).

Martin, A. D., Interpretation of residence time distribution data. Chemical Engineering Science, 55, 5907-5917 (2000).

Mishra, V. P., Dyster, K. N., Jaworski, Z., Nienow, A. W. and Mckemmie, J., A study of an up and down-pumping wide blade hydrofoil impeller: Part I. LAD measurements. Canadian Journal of Chemical Engineering, 76, 577-588 (1998).

Robinson, B. A. and Tester, J. W., Characterization of flow maldistribution using inlet-outlet tracer techniques: An application of internal residence time distributions. Chemical Engineering Science, 41, 469-483 (1986).

Trivedi, R. N. and Vasudeva, K., RTD for diffusion free laminar flow in helical coils. Chemical Engineering Science, 29, 2291-2295 (1974).

Turner, J. C. R., Perspectives in residence-time distributions. Chemical Engineering Science, 38, 1-4 (1982).

Xiao-chang, C., Ting-an, Z. and Qiu-yue, Z., Computational simulation of fluid dynamics in a tubular stirred reactor. Transactions of Nonferrous Metals Society of China, 19, 489-495 (2009).

Yablonskya, G. S., Constalesb, D. and Marinc, G. B., A new approach to diagnostics of ideal and non-ideal flow patterns: I, the concept of reactive-mixing index (REMI) analysis. Chemical Engineering Science, 64, 4875-4883 (2009).

Zwietering, T. N., The degree of mixing in continuous flow system. Chemical Engineering Science, 11, 1-15 (1959).